Published OnlineFirst January 24, 2011; DOI:10.1158/1078-0432.CCR-10-2393

Table 1. Association between clinicopathological variables and immunohistochemical results of $p14^{ARF}$, $p15^{INK4b}$, and $p16^{INK4a}$

Variable	No. of patients	$p14^{ARF}$ Preserved	$p14^{ARF}$ Decreased	$p14^{ARF}$ *P*	$p15^{INK4b}$ Preserved	$p15^{INK4b}$ Decreased	$p15^{INK4b}$ *P*	$p16^{INK4a}$ Preserved	$p16^{INK4a}$ Decreased	$p16^{INK4a}$ *P*
Clinical variables (primary cases, $n = 85$)										
Age, y										
<50	46	24	22	0.93	21	25	0.96	22	24	0.58
≥50	39	20	19		18	21		21	18	
Sex										
Male	45	26	19	0.24	22	23	0.56	20	25	0.23
Female	40	18	22		17	23		23	17	
NF1										
Present	33	16	17	0.63	14	19	0.61	15	18	0.45
Absent	52	28	24		25	27		28	24	
Site										
Extremity	38	20	18	0.98	17	21	0.29	19	19	0.77
Trunk wall	20	10	10		12	8		9	11	
Head and neck/ retroperitoneum/ visceral/spine	27	14	13		10	17		15	12	
Tumor depth										
Superficial	21	12	9	0.57	12	9	0.23	9	12	0.41
Deep	64	32	32		27	37		34	30	
Tumor size										
<5cm	24	15	9	0.21	16	8	0.015	15	9	0.17
≥5cm	61	29	32		23	38		28	33	
Adjuvant therapy										
Given	3	0	3	0.11	2	1	0.59	2	1	1.00
Not given	82	44	38		37	45		41	41	
AJCC staging										
I	26	14	12	0.21	14	12	0.63	14	12	0.81
II	41	21	20		16	25		22	19	
III	14	8	6		7	7		6	8	
IV	3	0	3		1	2		1	2	
Pathological variables (all cases, $n = 129$)										
Tumor necrosis										
No necrosis	63	37	26	0.30	39	24	0.17	34	29	0.28
<50%	52	23	29		24	28		31	21	
≥50%	14	7	7		6	8		5	9	
Mitotic counts										
0–9/10HPF	84	45	39	0.11	42	42	0.42	41	43	0.11
10–19/10HPF	17	5	12		9	8		9	8	
≥20/10HPF	28	17	11		18	10		20	8	
Ki-67–labeling index										
0%–9%	31	20	11	0.043	13	18	0.33	17	14	0.94
10%–29%	57	32	25		32	25		30	27	
≥30%	41	15	26		24	17		23	18	
Microvessel density										
<15/HPF	64	29	35	0.13	33	31	0.66	31	33	0.19
≥15/HPF	65	38	27		36	29		39	26	
Rhabdomyoblastic differentiation										
Present	16	5	11	0.074	8	8	0.77	7	9	0.37
Absent	113	62	51		61	52		63	50	
Epithelioid feature										
Present	8	2	6	0.11	2	6	0.091	4	4	0.80
Absent	121	65	56		67	54		66	55	
FNCLCC grading										
1	41	25	16	0.37	26	15	0.066	20	21	0.68
2	59	28	31		25	34		33	26	
3	29	14	15		18	11		17	12	

Published OnlineFirst January 24, 2011; DOI:10.1158/1078-0432.CCR-10-2393

(M 7240, 1:100; Dako) and anti-CD31 antibody (JC70A, 1:20; Dako) using the standard procedure. The Ki-67–labeling index and microvessel density (MVD) were calculated as described previously (32, 33).

Snap-frozen samples and WB analysis

Thirty-nine snap-frozen samples from 28 primary and 11 recurrent or metastatic tumors were obtained from the collection of our department. A total of 5 pairs of samples from the primary and the corresponding first recurrent or metastatic tumors were available for the purpose of comparison. Fresh tumor samples were carefully dissected for the tumors to exclude the surrounding normal tissue, and the samples were immediately frozen in liquid nitrogen and stored at −80°C.

To confirm the concordant immunohistochemical results, the expressions of $p14^{ARF}$, $p15^{INK4b}$, and $p16^{INK4a}$ protein were evaluated by WB analysis using snap-frozen samples as previously described (34). A total of 20 μg protein from each sample was used, and incubated with either anti-$p14^{ARF}$ (1:2,000 dilution), -$p15^{INK4b}$ (1:50), or -16^{INK4a} (1:200) antibodies. Anti-human actin mouse monoclonal antibody (1:5,000; Millipore) was used as an internal control. A frozen sample of normal skin tissue was used as an external positive control. Protein levels were standardized by actin, which was assigned an arbitrary level of 10, and the expression signal relative to this was taken as the expression value for each sample.

RNA extraction and quantitative RT-PCR

Total RNA was extracted from 39 frozen samples and a cell line as previously described (35). The MPNST cell line YST-1 (36), which expresses *CDKN2A* and *CDKN2B* mRNAs, was used as a positive control. Quantitative RT-PCR was carried out and the results were analyzed using predeveloped TaqMan assay reagents (*CDKN2A* Hs00233365_m1 and *CDKN2B* Hs00793225_m1 from Applied Biosystems, Life Technologies) and an ABI Prism 7700 Sequence Detection system (Applied Biosystems) as described previously (37). The standard curve was constructed with serial dilutions of YST-1 cell line samples. The obtained data were standardized by using data of the housekeeping gene, GAPDH (Hs99999905_m1). The final numerical value (V) in each sample was calculated as follows: V = *CDKN2A* or *CDKN2B* mRNA value/GAPDH mRNA value.

DNA extraction and analyses

Genomic DNA was isolated from 27 snap-frozen tumor materials by using standard proteinase K digestion and phenol/chloroform extraction as previously described (38).

Multiplex real-time PCR was carried out for detecting homozygous deletions (HD) of the *CDKN2A* gene. The primer sequences and PCR conditions were the same as those described previously (39). All primers, the TaqMan probes and the TaqMan Universal Master Mix were supplied by Applied Biosystems. A standard curve was constructed with serial dilutions of Human Genomic DNA (Clontech). Distilled water was used as a negative control in each PCR analysis. The *CDKN2A*/beta-actin ratios less than 40% were judged to represent HD according to the previous reports (39, 40).

Mutational analysis was carried out for exons 1 to 3 of the *CDKN2A* gene by PCR-SSCP and DNA sequencing. The primer sequences and PCR conditions were the same as those previously described (9). SSCP and the following DNA sequencing were carried out as described previously (41).

Methylation of the CpG island in the promoter region of the $p14^{ARF}$ and $p16^{INK4a}$ genes was determined by MSP. Bisulfite modification and MSP were carried out as described previously, using the same reagents, primers, and PCR conditions (9, 42).

Statistical analysis

The correlations between 2 dichotomous variables were evaluated by using either χ^2 test or, when appropriate, Fisher's exact test. The correlations among gene alteration, mRNA level, and protein expression were evaluated by Mann–Whitney U test. The difference in the proportion of $p14^{ARF}$-, $p15^{INK4b}$-, or $p16^{INK4a}$-positive cells between the primary and the recurrent tumors was evaluated by Wilcoxon signed-rank test. Survival curves were calculated with the Kaplan–Meier method, and the differences were compared by the log-rank test. Cox proportional hazards regression analysis was carried out to estimate the hazard ratios for positive risk factors for death. Statistical significance was defined as $P < 0.05$. Data analysis was carried out with the JMP statistical software package (version 8.0.2; SAS Institute Inc.).

Results

Immunohistochemistry

The representative examples of immunohistochemical staining are shown in Figure 1, and the correlations between $p14^{ARF}$, $p15^{INK4b}$, and $p16^{INK4a}$ immunoreactivity and the clinicopathological variables are summarized in Table 1. Almost all neurofibroma cells showed immunoreactivity for $p14^{ARF}$, $p15^{INK4b}$, and $p16^{INK4a}$, respectively, on the 12 paraffin-embedded specimens including a benign neurofibroma area with MPNST. $p14^{ARF}$ expression was decreased in 41of the 85 primary tumors (48%) and 62 of the 129 all specimens (48%). For the total group of 129 cases, decreased expression of $p14^{ARF}$ was frequently observed in the subgroup with a high Ki-67–labeling index ($P = 0.043$). $p15^{INK4b}$ expression was decreased in 46 of the 85 primary tumors (54%) and 60 of the 129 all specimens (47%). Decreased expression of $p15^{INK4b}$ was associated with large tumor size (more than 5 cm) in both the primary tumors ($P = 0.015$) and all specimens ($P = 0.0003$). $p16^{INK4a}$ expression was decreased in 42 of the 85 primary tumors (49%) and 59 of the 129 all specimens (46%). $p16^{INK4a}$ expression showed no significant correlation with any clinicopathological variables.

Published OnlineFirst January 24, 2011; DOI:10.1158/1078-0432.CCR-10-2393

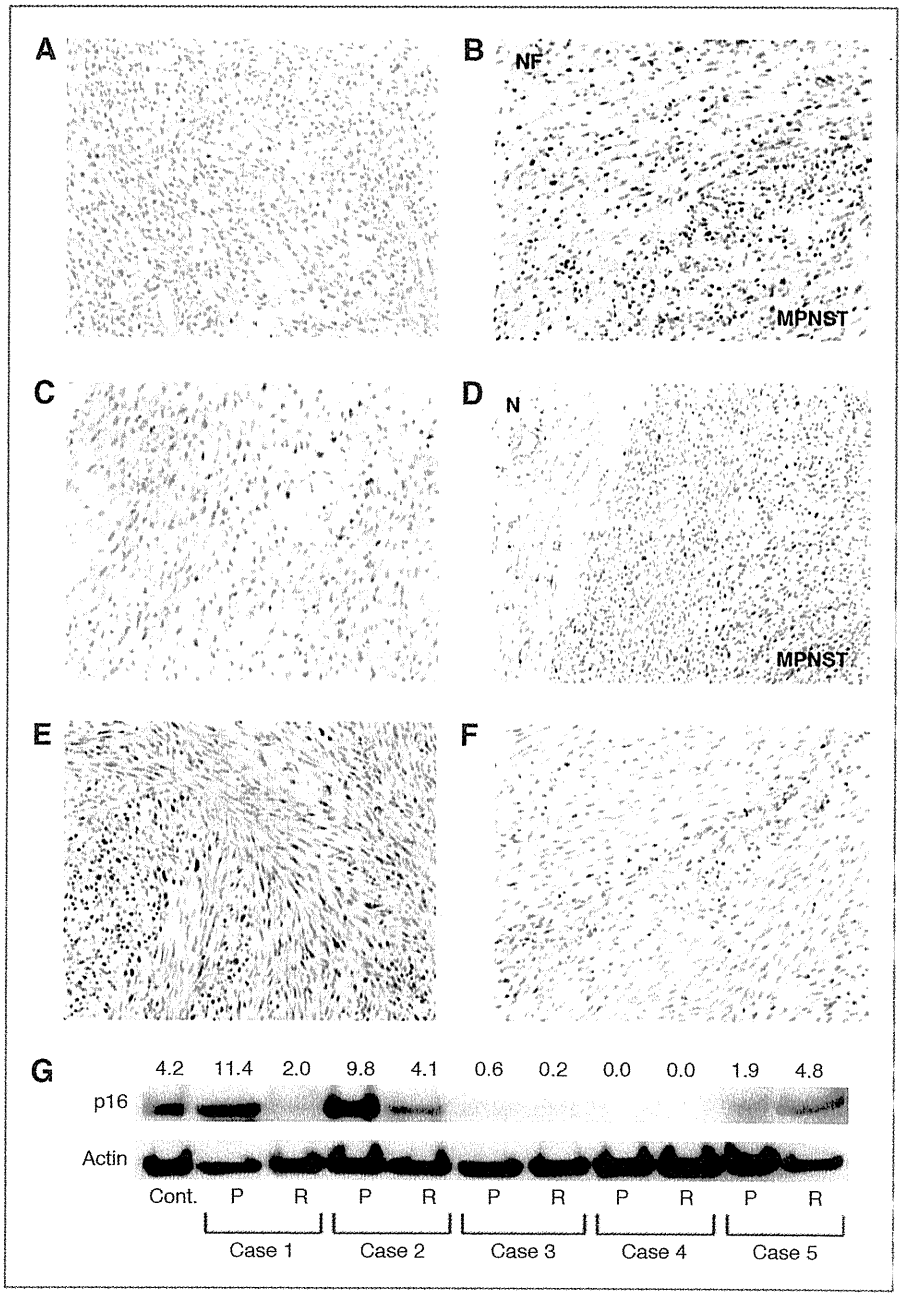

Figure 1. Representative examples of immunohistochemical staining. A, nuclear staining of $p14^{ARF}$ in MPNST. B, $p14^{ARF}$ expression in the gradual transition area from neurofibroma to MPNST. Most MPNST cells with plump nuclei were negative for $p14^{ARF}$ (MPNST, bottom right). Most spindle-shaped neurofibroma cells were positive for $p14^{ARF}$ (NF, top left). C, nuclear staining of $p15^{INK4b}$ in MPNST. D, decreased expression of $p15^{INK4b}$ in the MPNST area (MPNST, right). The expression was preserved in vascular endothelial cells and stromal cells in the surrounding normal tissue (N, left). E, nuclear staining of $p16^{INK4a}$ in MPNST. F, decreased expression of $p16^{INK4a}$ in MPNST. The expression was preserved in vascular endothelial cells. G, WB analysis of $p16^{INK4a}$ expression for a comparison between the primary and the corresponding recurrent tumors. The values at the top of the panel indicate the level of $p16^{INK4a}$ expression; this value was calculated relative to the actin intensity, which was assigned a value of 10. The expression level was decreased in the recurrent tumors of cases 1 and 2. A subtle decrease was observed in case 3. Case 4 shows no change, and case 5 shows an increase in $p16^{INK4a}$ expression. Cont.: positive control; P: primary; R: recurrent.

As for the difference in the IHC results between NF1-related and sporadic MPNSTs, $p14^{ARF}$ expression was decreased in 17 of the 33 NF1-related (52%) and 24 of the 52 sporadic cases (46%). $p15^{INK4b}$ expression was decreased in 19 of the 33 NF1-related (58%) and 27 of the 52 sporadic (52%) cases. $p16^{INK4a}$ expression was decreased in 18 of the 33 NF1-related (55%) and 24 of the 52 sporadic (46%) MPNSTs. There was no significant difference in $p14^{ARF}$, $p15^{INK4b}$, and $p16^{INK4a}$ expressions between NF1-related and sporadic MPNSTs.

A comparative analysis of the immunoreactivities for $p14^{ARF}$, $p15^{INK4b}$, and $p16^{INK4a}$ was carried out in the 18 pairs of the primary and the corresponding first recurrent or metastatic tumors. A decrease in the proportion of $p14^{ARF}$-, $p15^{INK4b}$-, and $p16^{INK4a}$-immunoreactive cells was observed in 10 (56%), 12 (67%), and 13 (72%) out of the 18 recurrent or metastatic tumors, respectively. There was no significant difference in positivity between the primary and the corresponding recurrent tumors; however, $p16^{INK4a}$ immunoreactivity showed a tendency

Published OnlineFirst January 24, 2011; DOI:10.1158/1078-0432.CCR-10-2393

Table 2. A comparison of $p14^{ARF}$, $p15^{INK4b}$, and $p16^{INK4a}$ expression results by IHC, WB, and qPCR

	$p14^{ARF}$			$p15^{INK4b}$			$p16^{INK4a}$		
Case no.	IHC	WB	qPCR	IHC	WB	qPCR	IHC	WB	qPCR
1	D	0	0.00	D	0	2.01	P	17.4	0.00
2	D	0	0.00	P	0.9	0.03	D	2.1	0.00
3	D	0	0.00	D	0	0.01	D	2	0.00
4	D	0	0.00	D	0	0.00	D	2.1	0.00
5	D	0	0.00	D	0	0.00	D	1.6	0.00
6	D	0	0.01	D	0	0.02	D	9.6	0.01
7	D	0	0.02	D	0	0.00	D	0	0.02
8	D	0	0.03	P	0	0.28	D	0.4	0.03
9	D	0	0.03	D	0	0.09	D	0.4	0.03
10	P	0	0.03	P	0	0.03	P	4.8	0.03
11	D	0	0.04	D	0	0.03	D	2.1	0.04
12	D	4.7	0.04	P	0	0.02	D	1.9	0.04
13	P	0	0.05	P	0	0.13	P	0.6	0.05
14	D	0	0.05	P	0	0.11	D	0	0.05
15	D	0	0.05	P	0	0.00	P	3.8	0.05
16	D	0	0.06	P	0	0.72	P	3	0.06
17	P	0	0.08	P	0	0.27	P	11.4	0.08
18	D	0	0.09	D	0	0.00	D	0.4	0.09
19	D	0	0.10	P	0	0.47	D	0.7	0.10
20	D	0	0.10	D	0	0.00	D	1.5	0.10
21	D	0	0.12	P	0	0.46	D	0.2	0.12
22	P	0	0.14	P	0	0.06	P	9.8	0.14
23	D	0	0.14	D	0	0.01	P	26.9	0.14
24	P	0	0.15	P	3.5	10.64	P	12	0.15
25	P	0	0.44	P	0	1.50	P	2.2	0.44
26	P	0	0.52	P	0	0.07	P	2.2	0.52
27	P	0	0.54	P	0	1.07	P	0.1	0.54
28	P	0	0.69	P	0	0.09	P	6	0.69
29	P	0	1.04	D	0	0.16	P	3	1.04
30	P	0	1.71	P	0	0.05	P	6.8	1.71
31	D	0	3.08	D	0	0.40	P	3.1	3.08
32	P	0.9	4.12	P	0	1.65	P	0.4	4.12
33	P	0	4.29	D	0	0.74	P	4.1	4.29
34	P	0	4.41	D	0	1.37	D	0	4.41
35	P	1.4	4.50	P	2.2	0.00	P	8.9	4.50
36	P	0	4.77	P	0	4.13	D	0.4	4.77
37	P	0	9.00	P	0	2.28	D	0	9.00
38	P	n.e.	9.72	P	n.e.	0.11	P	n.e.	9.72
39	P	3.6	11.23	P	0	6.13	D	2.2	11.23

NOTE: IHC: D, decreased expression; P, preserved expression; WB, number means expression value. 0, undetectable; n.e., not examined. qPCR: number means expression value. $p14^{ARF}$, $p16^{INK4a}$ mRNA: CDKN2A mRNA; $p15^{INK4b}$ mRNA: CDKN2B mRNA.

to be lower in the recurrent or metastatic tumors ($P = 0.12$).

Western blotting

Proteins of sufficient quality and quantity were successfully extracted from 38 out of the 39 frozen tumor specimens. WB analysis was carried out in 38 specimens using anti-$p14^{ARF}$, -$p15^{INK4b}$, and -$p16^{INK4a}$ antibodies. The $p14^{ARF}$ signal was detected in only 4 cases, and 3 of the 4 cases in which the $p14^{ARF}$ signal was detected on WB also presented preserved expression of this protein on IHC (Table 2). The $p15^{INK4b}$ signal was observed in only 3 cases, and all 3 cases in which the $p15^{INK4b}$ signal was detected on WB also presented preserved expression

Published OnlineFirst January 24, 2011; DOI:10.1158/1078-0432.CCR-10-2393

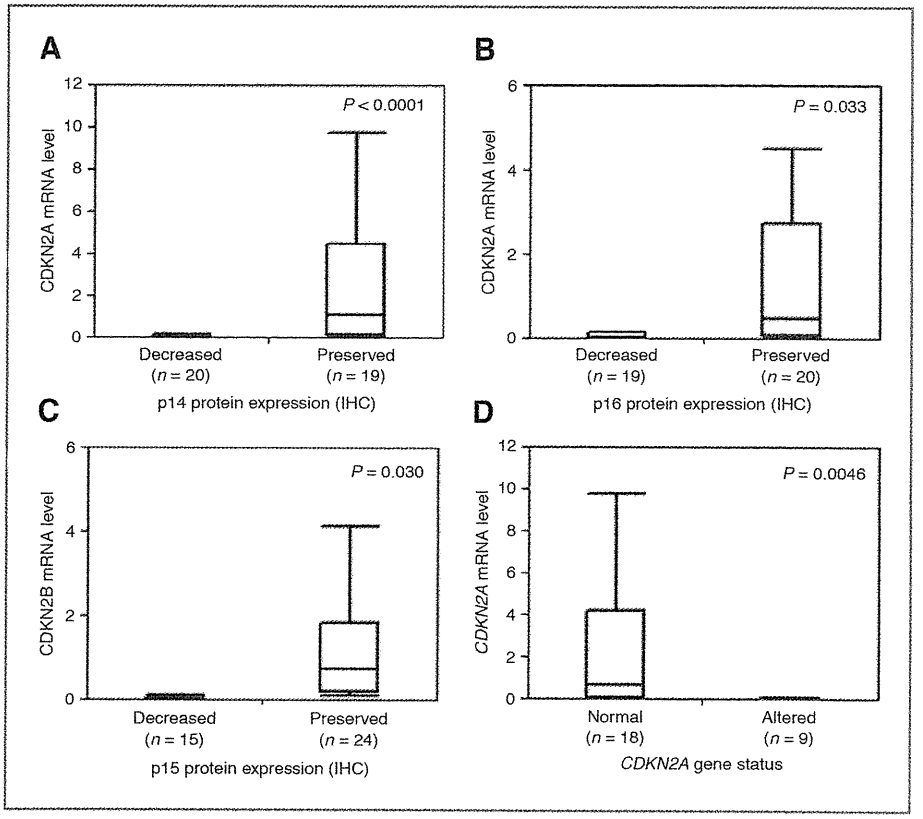

Figure 2. Association between the expression levels of *CDKN2A* mRNA and p14^{ARF} protein (A), *CDKN2A* mRNA and p16^{INK4a} protein (B), and *CDKN2B* mRNA and p15^{INK4b} protein (C). There were significant associations between the mRNA and protein expressions of *p14*^{ARF}, *p15*^{INK4b}, and *p16*^{INK4a}, respectively, with *P* values shown at the top right of the figures. D, association between mRNA levels and gene alterations of *CDKN2A*. The gene alterations were significantly correlated to the low levels of *CDKN2A* mRNA ($P = 0.0046$).

of this protein on IHC (Table 2). WB for the p16^{INK4a} protein showed a sufficient signal intensity to evaluate the relative expression levels in 34 of the 38 samples (Table 2). The relative expression level versus the actin expression level, which was assigned a value of 10, ranged from 0.0 to 26.9 (median 2.1). As for the comparison of the primary and the corresponding recurrent or metastatic tumors, p16^{INK4a} expression levels revealed a decrease in 2 of 5 cases, and a subtle decrease in 1 case (Fig. 1G). The expression levels of p16^{INK4a} by WB corresponded closely to the levels observed by IHC (Table 2).

mRNA expression assay by quantitative RT-PCR

The expression levels of *CDKN2A* mRNA (0.00–11.23, median 0.10) were significantly associated with both p14^{ARF} and p16^{INK4a} immunohistochemical protein expressions (Table 2, Fig. 2A and B). The expression levels of *CDKN2B* mRNA (0.00–10.64, median 0.095) were also correlated to p15^{INK4b} protein expressions (Table 2, Fig. 2C).

Gene alteration assessment by multiplex real-time PCR, PCR-SSCP, and MSP

Homozygous deletion (HD) of the *CDKN2A* gene was detected in 9 of 27 cases (33.3%) by multiplex real-time PCR assay. The remaining 18 cases without homozygous deletion were also analyzed by PCR-SSCP and MSP. No mutation was found in exons of *CDKN2A* by PCR-SSCP and the subsequent DNA sequencing (data not shown). MSP revealed that no methylation occurred in either the *p14*^{ARF} or *p16*^{INK4a} promoter region (data not shown). *CDKN2A* gene alterations represented by HD were significantly associated with low *CDKN2A* mRNA levels (Fig. 2D). All but one of the cases with HD in the *CDKN2A* gene showed decreased immunoreactivity for both p14^{ARF} and p16^{INK4a}.

Survival analysis

Univariate prognostic analysis revealed that decreased expressions of p14^{ARF} and p16^{INK4a} were significantly associated with decreased probability of overall survival, respectively (Table 3, Fig. 3A and B). Patients with decreased expression of p15^{INK4b} showed a strong tendency to have poor prognosis ($P = 0.051$; Table 3, Fig. 3C). Each of the following was associated with poor prognosis: tumor location in the trunk, tumor location in deep tissue, large tumor size (more than 5 cm), high Ki-67–labeling index (more than 30%), high histological grade (grade 2 or more), and advanced AJCC stage (stage II or higher).

Published OnlineFirst January 24, 2011; DOI:10.1158/1078-0432.CCR-10-2393

Table 3. Univariate analysis for overall survival

Variable	No. of patients	5-y survial rate	P
Age, y			
<50	45	51.4	0.41
≥50	37	53.2	
Sex			
Male	43	47.4	0.28
Female	39	57.4	
NF1			
Present	32	41.1	0.26
Absent	50	57.7	
Site			
Extremity	36	64.3	0.041
Trunk	46	42.5	
Tumor depth			
Superficial	20	78.6	0.004
Deep	62	43.4	
Tumor size			
<5cm	23	78.3	0.006
≥5cm	59	41.7	
Adjuvant therapy			
Given	3	50.0	0.47
Not given	79	52.0	
Tumor necrosis			
Absent	38	63.4	0.067
Present	44	42.3	
Mitotic counts			
0–9/10HPF	56	53.7	0.43
≥10/10HPF	26	47.1	
Ki-67–labeling index			
0%–29%	58	63.8	<0.001
≥30%	24	21.0	
Microvessel density			
<15/HPF	39	65.6	0.06
≥15/HPF	43	39.7	
Rhabdomyoblastic differentiation			
Present	10	33.8	0.20
Absent	72	54.5	
Epithelioid feature			
Present	5	20.0	0.11
Absent	77	54.6	
FNCLCC grading			
1	25	72.5	0.030
2 + 3	57	43.4	
AJCC staging			
I	25	72.5	0.030
II + III + IV	57	43.4	
$p14^{ARF}$ IHC			
Preserved	42	74.1	<0.001
Decreased	40	28.5	
$p15^{INK4b}$ IHC			
Preserved	38	67.9	0.051
Decreased	44	38.9	
$p16^{INK4a}$ IHC			
Preserved	41	68.9	0.002
Decreased	41	34.0	

A multivariate analysis carried out using variables that were related to poor prognosis in the univariate analysis revealed that tumor location in the trunk, tumor location in deep tissue, and decreased expressions of either $p14^{ARF}$ or $p16^{INK4a}$ persisted as independent risk factors for a poor outcome (Table 4).

In terms of $p14^{ARF}$ and $p16^{INK4a}$ expressions in the primary tumors, decreased expression of both $p14^{ARF}$ and $p16^{INK4a}$ was observed in 28 of the 82 patients (34.1%), whereas preserved expression of both was detected in 29 patients (35.4%; Table 5). A combined prognostic evaluation with grouping by $p14^{ARF}$ and $p16^{INK4a}$ expressions revealed that the 5-year overall survival rate of cases with a decrease in the expression of both proteins was 25.8%, whereas that of cases in which the expression of both proteins preserved was 83.3%, with the difference in the 2 values being statistically significant ($P < 0.001$).

There was an association between the prognosis and the number of inactivations among $p14^{ARF}$, $p15^{INK4b}$, and $p16^{INK4a}$; the cases with 2 or 3 inactivated genes showed a significantly more adverse prognosis than those with only 1 or no inactivated genes ($P < 0.001$; Table 5, Fig. 3D).

Finally, the prognostic significance of $p15^{INK4b}$ expression in the absence of $p16^{INK4a}$ was evaluated. Among the 41 cases with $p16^{INK4a}$ inactivation, 30 cases (73.2%) showed decreased expression of $p15^{INK4b}$, and the remaining 11 cases (26.8%) showed preserved expression of $p15^{INK4b}$ (Table 5). The 5-year overall survival rate of patients with coinactivation of $p15^{INK4b}$ and $p16^{INK4a}$ was 24.8%, whereas that of patients with preserved $p15^{INK4b}$ was 75.0%, which was significantly higher than that of coinactivated patients (Fig. 3E).

Discussion

Our univariate prognostic analysis of $p14^{ARF}$, $p15^{INK4b}$, and $p16^{INK4a}$ inactivation in MPNSTs revealed that each gene inactivation was significantly or almost significantly associated with poor prognosis. Furthermore, the prognostic importance of $p14^{ARF}$ and $p16^{INK4a}$ status in MPNSTs was reconfirmed by the multivariate analysis. A combined prognostic analysis showed that MPNSTs with inactivation of 2 or more genes among $p14^{ARF}$, $p15^{INK4b}$, and $p16^{INK4a}$ showed much worse prognosis than those with inactivation of 1 or no genes. The above results indicate that a synergistic effect of the combined deficiency for $p14^{ARF}$, $p15^{INK4b}$, and $p16^{INK4a}$ induced a further high-grade malignancy in MPNSTs. The results from this study contribute not only to estimation of the molecular pathophysiology of MPNST, but also to the improvement of clinical management of patients with MPNST through the provision of precise prognostic prediction.

The impact of $p15^{INK4b}$ inactivation in human cancers has been less clear than that of the $p14^{ARF}$ and $p16^{INK4a}$ inactivations (15). But recently, the significance of $p15^{INK4b}$

Published OnlineFirst January 24, 2011; DOI:10.1158/1078-0432.CCR-10-2393

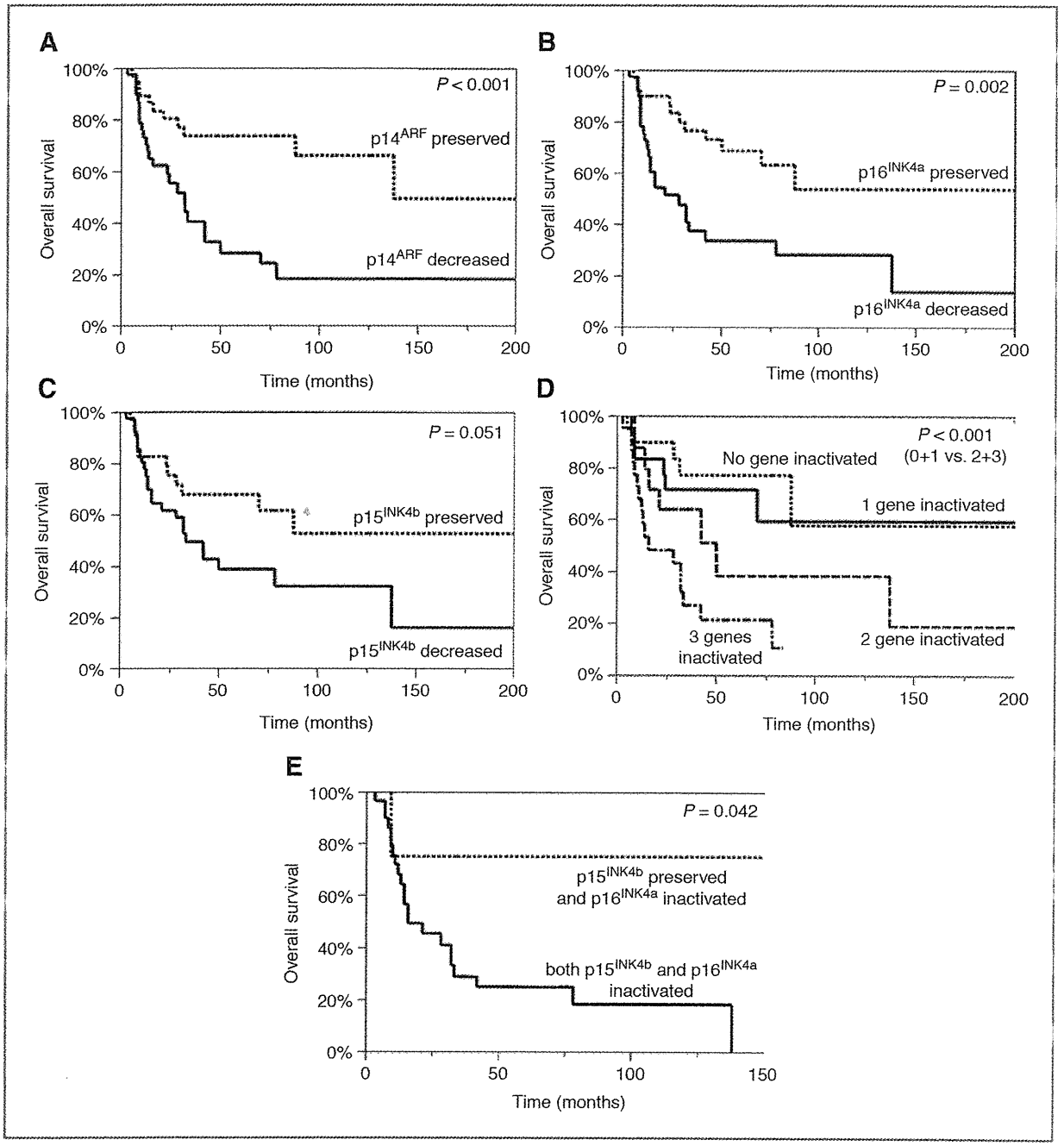

Figure 3. The Kaplan–Meier curves for overall survival according to $p14^{ARF}$ (A), $p16^{INK4a}$ (B), and $p15^{INK4b}$ (C) expressions. Decreased expressions of $p14^{ARF}$ and $p16^{INK4a}$ were associated with a decreased probability of overall survival, respectively, with *P* values shown at the top right of the figures. Decreased expression of $p15^{INK4b}$ showed a strong tendency toward association with poor prognosis ($P = 0.051$). D, the Kaplan–Meier curves for overall survival according to the number of inactivated genes among $p14^{ARF}$, $p15^{INK4b}$, and $p16^{INK4a}$. Patients with inactivation of 2 or more genes showed worse prognosis than those with 1 or no gene inactivated ($P < 0.001$). E, the Kaplan–Meier curves for overall survival in patients with $p16^{INK4a}$ inactivation according to the $p15^{INK4b}$ expression. Patients with preserved expression of $p15^{INb4b}$ in the absence of $p16^{INK4a}$ show better prognosis than the $p15^{INK4b}$ and $p16^{INK4a}$ coinactivated cases ($P = 0.042$).

inactivation in malignant tumors has got a lot of attention. The loss of *CDKN2B* encoding $p15^{INK4b}$ is observed in various types of malignant tumors, but the frequent loss of *CDKN2B* in human tumors could be explained by its juxtaposition to *CDKN2A*, in which proximity could lead to frequent codeletion. A recent study using a mouse model

Published OnlineFirst January 24, 2011; DOI:10.1158/1078-0432.CCR-10-2393

Table 4. Multivariate analysis for overall survival

Variable	Hazard ratio	95% CI	P
Site			
Extremity	1		
Trunk	2.08	1.44–2.99	0.042
Tumor depth			
Superficial	1		
Deep	3.93	2.05–7.56	0.025
Tumor size			
<5cm	1		
≥5cm	1.26	0.71–2.25	0.69
Ki-67–labeling index			
0%–29%	1		
≥30%	1.36	0.89–2.08	0.47
FNCLCC grading			
1	1		
2 + 3	1.83	1.15–2.92	1.00
AJCC staging			
I	1		
II + III + IV	1	1–1	1.00
$p14^{ARF}$ IHC			
Preserved	1		
Decreased	2.72	1.75–4.21	0.021
$p16^{INK4a}$ IHC			
Preserved	1		
Decreased	2.21	1.52–3.22	0.034

has proposed the interesting hypothesis that $p15^{INK4b}$ functions as a critical tumor suppressor in the absence of $p16^{INK4a}$ (15). In human tumors, the tumor-suppressive effect of $p15^{INK4b}$ in the setting of $p16^{INK4a}$ inactivation has not been investigated well. This is the first report evaluating the prognostic role of $p15^{INK4b}$ in the absence of $p16^{INK4a}$ in MPNSTs. Our prognostic analysis of $p16^{INK4a}$-inactivated cases showed that $p15^{INK4b}$-preserved cases showed significantly better prognosis than $p15^{INK4b}$-inactivated cases. This finding indirectly supports the hypothesis that $p15^{INK4b}$ provides a critical backup function for $p16^{INK4a}$ in MPNSTs. In addition, it may provide an explanation for the frequent loss of the complete *CDKN2B–CDKN2A* locus in human high-grade malignancies, including MPNST (15, 43).

Here we revealed the frequency of inactivation of $p14^{ARF}$, $p15^{INK4b}$, and $p16^{INK4a}$ in MPNSTs by a large-scale clinicopathological study with multiple methods. Inactivation of $p14^{ARF}$, $p15^{INK4b}$, and $p16^{INK4a}$ was observed in 50%, 49%, and 53% of MPNSTs, respectively. In previous studies, the frequency of $p14^{ARF}$, $p15^{INK4b}$, and $p16^{INK4a}$ inactivation in MPNSTs has been a controversial issue. Some papers have stated that $p16^{INK4a}$ inactivation in neurofibroma is a critical process in progression to MPNST, and $p16^{INK4a}$ is inactivated in almost all MPNSTs (18, 19, 44). On the other hand, some recent papers have indicated that 9p21-related genes including $p16^{INK4a}$ are inactivated in only half of all cases of MPNST (24, 43, 45). Our data support the latter statement: we found that inactivation of the $p14^{ARF}$, $p15^{INK4b}$, and $p16^{INK4a}$ genes was involved in high-grade malignant transformation in about half of the MPNSTs studied.

CDKN2A is known to exhibit more HDs than other recessive cancer genes in various types of cancers (46). This may be because it is adjacent to a large gene desert and therefore HDs are associated with less negative selection (46). Our study showed that HD of *CDKN2A* was detected in 33.3% of the cases, whereas neither point mutation of *CDKN2A* nor methylation of the $p14^{ARF}$ and $p16^{INK4a}$ promoter regions was detected. In addition to our study, several other authors have investigated gene alterations of *CDKN2A* in MPNSTs (16–23, 42–44, 47). According to their reports, HD is the predominant cause of inactivation of the 9p21 locus in MPNSTs, and the rate

Table 5. Combinational prognostic analysis of $p14^{ARF}$, $p15^{INK4b}$, and $p16^{INK4a}$ expressions

Variables			No. of patients	5-y survial rate	P
Combinational prognostic analysis of $p14^{ARF}$ and $p16^{INK4a}$ expressions	$p14^{ARF}$	$p16^{INK4a}$			
	D	D	28 (34.1%)	25.8	<0.001 (DD vs. PP)
	D	P	12 (14.6%)	31.3	
	P	D	13 (15.9%)	51.1	
	P	P	29 (35.4%)	83.3	
The number of inactivated genes among $p14^{ARF}$, $p15^{INK4b}$, and $p16^{INK4a}$		0	20 (24.4%)	77.1	<0.001 (0 + 1 vs. 2 + 3)
		1	22 (26.8%)	71.4	
		2	17 (20.7%)	38.2	
		3	23 (28.0%)	21.6	
Prognostic effect of $p15^{INK4b}$ expression in the absence of $p16^{INK4a}$	$p15^{INK4b}$	$p16^{INK4a}$			
	D	D	30 (73.2%)	24.8	0.042
	P	D	11 (26.8%)	75	

NOTE: D, decreased; P, preserved; DD, decreased in both $p14^{ARF}$ and $p16^{INK4a}$; PP, preserved in both $p14^{ARF}$ and $p16^{INK4a}$.

Published OnlineFirst January 24, 2011; DOI:10.1158/1078-0432.CCR-10-2393

of HD ranges from 7.1% to 56.5% (16–20, 22, 43, 44, 47). Point mutation of *CDKN2A* has been reported in only 1 MPNST case (17). Methylation of the $p14^{ARF}$ and $p16^{INK4a}$ promoter regions has been reported in only 2 cases (7.7% of the investigated cases), respectively (43). Our results are basically consistent with those of the previous reports, and indicate that the main alteration causing *CDKN2A* gene inactivation is HD rather than point mutation or methylation of the promoter regions in MPNSTs.

NF1-related MPNST has an *NF1* gene dysfunction leading to an excessive activation of the Ras signal pathway, whereas sporadic MPNST does not always show an *NF1* gene dysfunction (48). The pathogenesis of MPNST is a fascinating subject, because both NF1-related and sporadic MPNSTs show similar histological findings and molecular characteristics despite their difference in genetic background. Our study showed that there was no significant difference in the expressions of $p14^{ARF}$, $p15^{INK4b}$, and $p16^{INK4a}$ between NF1-related and sporadic MPNSTs. Perrone and colleagues reported that inactivation of 1 or more 9p21-related genes detected by RT-PCR was found in 11 of 14 NF1-related (78%) and 9 of 12 sporadic (75%) cases, respectively (43). They concluded that the inactivation profile of 9p21-related genes showed no significant difference between NF1-related and sporadic MPNSTs. Our findings were basically consistent with those of this previous report.

In summary, we carried out a comprehensive analysis of $p14^{ARF}$, $p15^{INK4b}$, and $p16^{INK4a}$ expressions in MPNSTs. Inactivation of $p14^{ARF}$, $p15^{INK4b}$, and $p16^{INK4a}$ was associated with poor prognosis, respectively, and a combined inactivation of them leaded to worse prognosis in MPNSTs. We conclude that a combined evaluation of $p14^{ARF}$, $p15^{INK4b}$, and $p16^{INK4a}$ status provides useful prognostic information for patients with MPNSTs.

Acknowledgments

The authors appreciate for the technical supports from Ms. Tateishi and the Research Support Center, Graduate School of Medical Sciences, Kyushu University. They also appreciate KN International for revising the English used in this article.

Grant Support

Y. Oda is supported by a Grant-in-Aid for Scientific Research (B; grant no. 21390107) from the Japan Society for the Promotion of Science, Tokyo, Japan.

The costs of publication of this article were defrayed in part by the payment of page charges. This article must therefore be hereby marked *advertisement* in accordance with 18 U.S.C. Section 1734 solely to indicate this fact.

Received September 6, 2010; revised December 28, 2010; accepted January 10, 2011; published OnlineFirst January 24, 2011.

References

1. Anghileri M, Miceli R, Fiore M, Mariani L, Ferrari A, Mussi C, et al. Malignant peripheral nerve sheath tumors: prognostic factors and survival in a series of patients treated at a single institution. Cancer 2006;107:1065–74.
2. Ducatman BS, Scheithauer BW, Piepgras DG, Reiman HM, Ilstrup DM. Malignant peripheral nerve sheath tumors. A clinicopathologic study of 120 cases. Cancer 1986;57:2006–21.
3. Cichowski K, Shih TS, Schmitt E, Santiago S, Reilly K, McLaughlin ME, et al. Mouse models of tumor development in neurofibromatosis type 1. Science 1999;286:2172–6.
4. Vogel KS, Klesse LJ, Velasco-Miguel S, Meyers K, Rushing EJ, Parada LF. Mouse tumor model for neurofibromatosis type 1. Science 1999;286:2176–9.
5. Hummel TR, Jessen W, Miller SC, Kluwe L, Mautner V, Wallace MR, et al. Gene expression analysis identifies potential biomarkers of neurofibromatosis type 1 including adrenomedullin. Clin Cancer Res . 2010;16:5048–57.
6. Levy P, Ripoche H, Laurendeau I, Lazar V, Ortonne N, Parfait B, et al. Microarray-based identification of tenascin C and tenascin XB, genes possibly involved in tumorigenesis associated with neurofibromatosis type 1. Clin Cancer Res 2007;13:398–407.
7. Sordillo PP, Helson L, Hajdu SI, Magill GB, Kosloff C, Golbey RB, et al. Malignant schwannoma—clinical characteristics, survival, and response to therapy. Cancer 1981;47:2503–9.
8. Hruban RH, Shiu MH, Senie RT, Woodruff JM. Malignant peripheral nerve sheath tumors of the buttock and lower extremity. A study of 43 cases. Cancer 1990;66:1253–65.
9. Kawaguchi K, Oda Y, Saito T, Yamamoto H, Tamiya S, Takahira T, et al. Mechanisms of inactivation of the p16INK4a gene in leiomyosarcoma of soft tissue: decreased p16 expression correlates with promoter methylation and poor prognosis. J Pathol 2003;201:487–95.
10. Oda Y, Yamamoto H, Takahira T, Kobayashi C, Kawaguchi K, Tateishi N, et al. Frequent alteration of p16(INK4a)/p14(ARF) and p53 pathways in the round cell component of myxoid/round cell liposarcoma: p53 gene alterations and reduced p14(ARF) expression both correlate with poor prognosis. J Pathol 2005;207:410–21.
11. Perrone F, Tamborini E, Dagrada GP, Colombo F, Bonadiman L, Albertini V, et al. 9p21 locus analysis in high-risk gastrointestinal stromal tumors characterized for c-kit and platelet-derived growth factor receptor alpha gene alterations. Cancer 2005;104:159–69.
12. Cao J, Zhou J, Gao Y, Gu L, Meng H, Liu H, et al. Methylation of p16 CpG island associated with malignant progression of oral epithelial dysplasia: a prospective cohort study. Clin Cancer Res 2009;15:5178–83.
13. Hallor KH, Staaf J, Bovee JV, Hogendoorn PC, Cleton-Jansen AM, Knuutila S, et al. Genomic profiling of chondrosarcoma: chromosomal patterns in central and peripheral tumors. Clin Cancer Res 2009;15:2685–94.
14. Latres E, Malumbres M, Sotillo R, Martin J, Ortega S, Martin-Caballero J, et al. Limited overlapping roles of P15(INK4b) and P18(INK4c) cell cycle inhibitors in proliferation and tumorigenesis. EMBO J 2000;19:3496–506.
15. Krimpenfort P, Ijpenberg A, Song JY, Van Der Valk M, Nawijn M, Zevenhoven J, et al. p15Ink4b is a critical tumour suppressor in the absence of p16Ink4a. Nature 2007;448:943–6.
16. Berner JM, Sorlie T, Mertens F, Henriksen J, Saeter G, Mandahl N, et al. Chromosome band 9p21 is frequently altered in malignant peripheral nerve sheath tumors: studies of CDKN2A and other genes of the pRB pathway. Genes Chromosomes Cancer 1999;26:151–60.
17. Kourea HP, Orlow I, Scheithauer BW, Cordon-Cardo C, Woodruff JM. Deletions of the INK4A gene occur in malignant peripheral nerve sheath tumors but not in neurofibromas. Am J Pathol 1999;155:1855–60.
18. Nielsen GP, Stemmer-Rachamimov AO, Ino Y, Moller MB, Rosenberg AE, Louis DN. Malignant transformation of neurofibromas in neurofibromatosis 1 is associated with CDKN2A/p16 inactivation. Am J Pathol 1999;155:1879–84.
19. Birindelli S, Perrone F, Oggionni M, Lavarino C, Pasini B, Vergani B, et al. Rb and TP53 pathway alterations in sporadic and NF1-related

Published OnlineFirst January 24, 2011; DOI:10.1158/1078-0432.CCR-10-2393

malignant peripheral nerve sheath tumors. Lab Invest 2001;81:833–44.
20. Perry A, Kunz SN, Fuller CE, Banerjee R, Marley EF, Llapis H, et al. Differential NF1, p16, and EGFR patterns by interphase cytogenetics (FISH) in malignant peripheral nerve sheath tumor (MPNST) and morphologically similar spindle cell neoplasms. J Neuropathol Exp Neurol 2002;61:702–9.
21. Upadhyaya M, Han S, Consoli C, Majounie E, Horan M, Thomas NS, et al. Characterization of the somatic mutational spectrum of the neurofibromatosis type 1 (NF1) gene in neurofibromatosis patients with benign and malignant tumors. Hum Mutat 2004;23:134–46.
22. Holtkamp N, Malzer E, Zietsch J, Okuducu AF, Mucha J, Mawrin C, et al. EGFR and erbB2 in malignant peripheral nerve sheath tumors and implications for targeted therapy. Neuro Oncol 2008;10:946–57.
23. Spurlock G, Knight SJ, Thomas N, Kiehl TR, Guha A, Upadhyaya M. Molecular evolution of a neurofibroma to malignant peripheral nerve sheath tumor (MPNST) in an NF1 patient: correlation between histopathological, clinical and molecular findings. J Cancer Res Clin Oncol 2010;136:1869–80.
24. Mantripragada KK, Spurlock G, Kluwe L, Chuzhanova N, Ferner RE, Frayling IM, et al. High-resolution DNA copy number profiling of malignant peripheral nerve sheath tumors using targeted microarray-based comparative genomic hybridization. Clin Cancer Res 2008;14:1015–24.
25. Scheithauer BW, Louis DN, Hunter S, Woodruff JM, Antonescu CR. Malignant peripheral nerve sheath tumour (MPNST). In:Louis DN, Ohgaki H, Wiestler OD, editors. WHO Classification of Tumours of the Central Nervous System. Lyon, France: IARC; 2007. p. 160–2.
26. Malignant tumors of the peripheral nerves. In:Weiss SW, Goldblum JR, editors. Enzinger and Weiss's Soft Tissue Tumors. 5th ed. St. Louis, MO: Mosby; 2008. p. 903–44.
27. Neurofibromatosis. Conference statement. National Institutes of Health Consensus Development Conference. Arch Neurol 1988;45:575–8.
28. Guillou L, Coindre JM, Bonichon F, Nguyen BB, Terrier P, Collin F, et al. Comparative study of the National Cancer Institute and French Federation of Cancer Centers Sarcoma Group grading systems in a population of 410 adult patients with soft tissue sarcoma. J Clin Oncol 1997;15:350–62.
29. Edge SB, Byrd DR, Compton CC, Fritz AG, Greene FL, Trotti AIII, editors. AJCC Cancer Staging Manual. 7th ed. New York: Springer; 2010.
30. Iwasa A, Oda Y, Kurihara S, Ohishi Y, Yasunaga M, Nishimura I, et al. Malignant transformation of mature cystic teratoma to squamous cell carcinoma involves altered expression of p53- and p16/Rb-dependent cell cycle regulator proteins. Pathol Int 2008;58:757–64.
31. Child FJ, Scarisbrick JJ, Calonje E, Orchard G, Russell-Jones R, Whittaker SJ. Inactivation of tumor suppressor genes p15(INK4b) and p16(INK4a) in primary cutaneous B cell lymphoma. J Invest Dermatol 2002;118:941–8.
32. Kobayashi C, Oda Y, Takahira T, Izumi T, Kawaguchi K, Yamamoto H, et al. Chromosomal aberrations and microsatellite instability of malignant peripheral nerve sheath tumors: a study of 10 tumors from nine patients. Cancer Genet Cytogenet 2006;165:98–105.
33. Hemmerlein B, Galuschka L, Putzer N, Zischkau S, Heuser M. Comparative analysis of COX-2, vascular endothelial growth factor and microvessel density in human renal cell carcinomas. Histopathology 2004;45:603–11.
34. Kohashi K, Oda Y, Yamamoto H, Tamiya S, Matono H, Iwamoto Y, et al. Reduced expression of SMARCB1/INI1 protein in synovial sarcoma. Mod Pathol 23;981–90.
35. Kobayashi C, Oda Y, Takahira T, Izumi T, Kawaguchi K, Yamamoto H, et al. Aberrant expression of CHFR in malignant peripheral nerve sheath tumors. Mod Pathol 2006;19:524–32.
36. Nagashima Y, Ohaki Y, Tanaka Y, Sumino K, Funabiki T, Okuyama T, et al. Establishment of an epithelioid malignant schwannoma cell line (YST-1). Virchows Arch B Cell Pathol Incl Mol Pathol 1990;59:321–7.
37. Matsuura S, Oda Y, Matono H, Izumi T, Yamamoto H, Tamiya S, et al. Overexpression of A disintegrin and metalloproteinase 28 is correlated with high histologic grade in conventional chondrosarcoma. Hum Pathol. 41:343–51.
38. Kohashi K, Oda Y, Yamamoto H, Tamiya S, Oshiro Y, Izumi T, et al. SMARCB1/INI1 protein expression in round cell soft tissue sarcomas associated with chromosomal translocations involving EWS: a special reference to SMARCB1/INI1 negative variant extraskeletal myxoid chondrosarcoma. Am J Surg Pathol 2008;32:1168–74.
39. Carter TL, Reaman GH, Kees UR. INK4A/ARF deletions are acquired at relapse in childhood acute lymphoblastic leukaemia: a paired study on 25 patients using real-time polymerase chain reaction. Br J Haematol 2001;113:323–8.
40. Berggren P, Kumar R, Sakano S, Hemminki L, Wada T, Steineck G, et al. Detecting homozygous deletions in the CDKN2A(p16(INK4a))/ARF(p14(ARF)) gene in urinary bladder cancer using real-time quantitative PCR. Clin Cancer Res 2003;9:235–42.
41. Saito T, Oda Y, Sakamoto A, Tamiya S, Kinukawa N, Hayashi K, et al. Prognostic value of the preserved expression of the E-cadherin and catenin families of adhesion molecules and of beta-catenin mutations in synovial sarcoma. J Pathol 2000;192:342–50.
42. Kawaguchi K, Oda Y, Saito T, Yamamoto H, Takahira T, Kobayashi C, et al. DNA hypermethylation status of multiple genes in soft tissue sarcomas. Mod Pathol 2006;19:106–14.
43. Perrone F, Tabano S, Colombo F, Dagrada G, Birindelli S, Gronchi A, et al. p15INK4b, p14ARF, and p16INK4a inactivation in sporadic and neurofibromatosis type 1-related malignant peripheral nerve sheath tumors. Clin Cancer Res 2003;9:4132–8.
44. Agesen TH, Florenes VA, Molenaar WM, Lind GE, Berner JM, Plaat BE, et al. Expression patterns of cell cycle components in sporadic and neurofibromatosis type 1-related malignant peripheral nerve sheath tumors. J Neuropathol Exp Neurol 2005;64:74–81.
45. Zhou H, Coffin CM, Perkins SL, Tripp SR, Liew M, Viskochil DH. Malignant peripheral nerve sheath tumor: a comparison of grade, immunophenotype, and cell cycle/growth activation marker expression in sporadic and neurofibromatosis 1-related lesions. Am J Surg Pathol 2003;27:1337–45.
46. Bignell GR, Greenman CD, Davies H, Butler AP, Edkins S, Andrews JM, et al. Signatures of mutation and selection in the cancer genome. Nature 463:893–8.
47. Orlow I, Drobnjak M, Zhang ZF, Lewis J, Woodruff JM, Brennan MF, et al. Alterations of INK4A and INK4B genes in adult soft tissue sarcomas: effect on survival. J Natl Cancer Inst 1999;91:73–9.
48. Grobmyer SR, Reith JD, Shahlaee A, Bush CH, Hochwald SN. Malignant Peripheral Nerve Sheath Tumor: molecular pathogenesis and current management considerations. J Surg Oncol 2008;97:340–9.

Histopathology 2011, **59**, 368–375. DOI: 10.1111/j.1365-2559.2011.03945.x

Abnormalities of the Wnt/β-catenin signalling pathway induce tumour progression in sporadic desmoid tumours: correlation between β-catenin widespread nuclear expression and VEGF overexpression

Hiroshi Matono,[1] Sadafumi Tamiya,[1] Ryohei Yokoyama,[1] Tsuyoshi Saito, Yukihide Iwamoto,[2] Masazumi Tsuneyoshi[1] & Yoshinao Oda[1]

Department of Anatomic Pathology, Graduate School of Medical Sciences, Kyushu University, Fukuoka, Japan, [1]Division of Orthopaedic Surgery, National Kyushu Cancer Center, Fukuoka, Japan, and [2]Department of Orthopaedic Surgery, Graduate School of Medical Sciences, Kyushu University, Fukuoka, Japan

Date of Submission 28 December 2009
Accepted for publication 10 August 2010

Matono H, Tamiya S, Yokoyama R, Saito T, Iwamoto Y, Tsuneyoshi M & Oda Y
(2011) *Histopathology* **59**, 368–375

Abnormalities of the Wnt/β-catenin signalling pathway induce tumour progression in sporadic desmoid tumours: correlation between β-catenin widespread nuclear expression and VEGF overexpression

Aims: To analyse the correlation between β-catenin and vascular endothelial growth factor (VEGF) in sporadic desmoid tumours.

Methods and results: The correlation between β-catenin aberrant expression and VEGF overexpression was examined and microvessel density (MVD) assessed by immunohistochemical expression of CD31 in 74 samples (63 primary and 11 recurrent samples, 63 patients) of sporadic desmoid tumours without familial adenomatous polyposis (FAP). β-*catenin* gene mutation and mRNA expression of *VEGF* was then examined by quantitative reverse transcriptase–polymerase chain reaction (RT–PCR). There was a statistically significant correlation between widespread nuclear expression of β-catenin and overexpression of VEGF in all desmoid tumours ($P = 0.04$, Fisher's exact test). MVD in recurrent tumours was significantly higher than that in primary tumours.

Conclusions: Abnormalities of β-catenin and VEGF overexpression play an important role in the neoplastic progression of sporadic desmoid tumours.

Keywords: β-catenin, desmoid tumour, vascular endothelial growth factor, Wnt signalling

Abbreviations: FAP, familial adenomatous polyposis; MVD, microvessel density; RT–PCR, reverse transcriptase–polymerase chain reaction; SSCP, single-strand conformation polymorphism; VEGF, vascular endothelial growth factor

Introduction

Desmoid tumours (desmoid-type fibromatoses) are uncommon soft tissue tumours. These tumours consist of fibroblastic/myofibroblastic cells with no atypia and recur frequently after surgical resection.[1] In desmoid tumours, Wnt/β-catenin plays an important role in tumorigenesis or tumour development.[2] Indeed, the role of Wnt/β-catenin signalling has been established in a number of tumour types. We have demonstrated recently that widespread β-catenin nuclear expression correlates with matrix metalloproteinase-7 (MMP-7) overexpression in sporadic desmoid tumours.[3] Moreover, in the β-*catenin* mutated group, *MMP-7 mRNA* expression was significantly higher than that of the β-*catenin* wild-type group.[3] However, we could not elucidate the definitive factors affecting local

Address for correspondence: Y. Oda, Department of Anatomic Pathology, Pathological Sciences, Graduate School of Medical Sciences, Kyushu University, Maidashi 3-1-1, Higashi-ku, Fukuoka 812-8582, Japan. e-mail: oda@surgpath.med.kyushu-u.ac.jp

recurrence. Recently, Lazar *et al.*[4] reported that β-*catenin* mutation in codon 45 correlated with increased desmoid tumour recurrence. Angiogenesis is a critical process for tumour growth and invasion.[5] Yokoyama *et al.*[6] reported that slit-like blood vessels lying in proliferated fibrous tissue were characteristic in desmoid tumours, and the number of vessels <20 μm in diameter in the central portion of the tumour was greater in patients with recurrences. Angiogenesis is considered to be correlated with recurrence and to be regulated by vascular endothelial growth factor (VEGF), which may also be a target gene of the Wnt/β-catenin signalling pathway.[7] In this study, to test the hypothesis that accumulated β-catenin within nuclei could affect regulation of the target genes, we examined the correlation between the immunohistochemical expressions of β-catenin and VEGF, which is a target gene product of the Wnt/β-catenin signalling pathway, in sporadic desmoid tumours without familial adenomatous polyposis (FAP). We also examined microvessel density which is correlated with angiogenesis, comparing that in primary tumours with that in recurrent tumours. Moreover, we searched for genetic alteration of β-*catenin* genes in 33 frozen samples (33 samples from 22 cases). We further examined mRNA expressions of *VEGF* in frozen samples by quantitative reverse transcription–polymerase chain reaction (RT–PCR) and compared the mRNA expression levels with the β-*catenin* mutation status.

Materials and methods

MATERIALS

From materials registered in the Department of Anatomic Pathology, Graduate School of Medical Sciences, Kyushu University, Japan between 1979 and 2006, 74 formalin-fixed, paraffin-embedded samples of desmoid tumours were retrieved from 63 patients to use in the immunohistochemical study. All patients had been treated surgically by marginal or wide resection. These included 22 male and 41 female patients with a mean age of 34.2 years (range 0–76 years), as shown in Table 1. The tumour location was divided into three groups: abdominal desmoid in 12 patients (three male and nine female patients), intra-abdominal desmoid in nine patients (three male and six female patients) and extra-abdominal desmoid in 42 patients (16 male and 26 female patients). The sites of the extra-abdominal desmoids are summarized in Table 2. Sixty-three samples (12 abdominal, nine intra-abdominal and 42 extra-abdominal) were primary tumours, and 11 samples (five patients, all extra-abdominal) were recurrent tumours at the time of diagnosis, as shown in Table 3. The diagnosis of all cases was based on light microscopic examination of haematoxylin and eosin stained tissue sections, according to the recent World Health Organization classification.[8]

Table 1. Desmoid tumours

	Abdominal	Intra-abdominal	Extra-abdominal	Total
Female	9	6	26	41
Male	3	3	16	22
Age mean (range, years)	39.4(25–74)	38.7(6–65)	31.8(0–76)	34.2
Total patients	12	9	42	63

For molecular analysis, 33 fresh frozen samples of desmoid tumours from 22 patients were used and three samples of normal skeletal muscle tissue as controls. Frozen material included 22 primary samples (one abdominal, four intra-abdominal and 17 extra-abdominal) and 11 recurrent samples (five patients, all extra-abdominal).

IMMUNOHISTOCHEMISTRY

Immunohistochemiistry was performed using anti-β-catenin mouse monoclonal antibody (dilution 1:200; Transduction Laboratories, Lexington, KY,

Table 2. Tumour site in extra-abdominal desmoids

Anatomical site	*n*
Extremity	21
Shoulder	8
Thigh	7
Upper arm	4
Others	2
Trunk	12
Buttock	5
Chest wall	4
Back	3
Head and neck	9
Total	42

Table 3. Recurrent cases

Case	Age (primary)	Gender	Site	No. of times
1	23	Female	Left thigh	5
2	34	Male	Left thigh	3
3	29	Female	Right thigh	1
4	39	Male	Right buttock	1
5	13	Male	Right lower leg	1

USA), anti-VEGF mouse polyclonal antibody (dilution 1:400; Santa Cruz Biotechnology, Santa Cruz, CA, USA) and anti-CD31 mouse monoclonal antibody (dilution 1:20; Dako, Glostrup, Denmark). Each section was considered to demonstrate widespread β-catenin nuclear staining (aberrant staining) if more than 50% of the tumour cells showed a nuclear immunoreactivity, and each section was considered to demonstrate VEGF overexpression if more than 10% of the tumour cells showed cytoplasmic positivity.[9,10]

MICROVESSEL DENSITY

The degree of angiogenesis was determined by the number of microvessels in the most vascularized areas within the tumour ('hot spot') according to the methods of Kaya *et al.*[11] The number of CD31-positive vessels was counted in four selected hot spots at a high magnification (×400; 0.26 mm^2) field. The mean value of the four independent readings of the same specimen was calculated, and microvessel density (MVD) was defined as the mean count of microvessels per 0.26 mm^2 field area. We compared MVD in primary tumours with that in recurrent tumours and evaluated whether MVD was correlated with VEGF expression in desmoid tumours.

β-*CATENIN* GENE MUTATION

Genomic DNA was purified from 33 specimens (33 samples from 22 cases) of frozen materials using standard proteinase K digestion and phenol/chloroform extraction after homogenization. PCR single-strand conformation polymorphism (SSCP) was carried out for the entire region of the β-*catenin* gene exon 3 using pairs of primers, G-forward (5′-CCAA TCTACTAATGCTAATACTG-3′) and G-reverse (5′-CTG CATTCTGACTTTCAGTAAGG-3′) for genomic DNA, and C-forward (5′-CCAGCGTGGACAATGGCTAC-3′) and C-reverse (5′-TGAGCTCGAGTCATTGCATAC-3′) for cDNA amplification.[12] PCR was carried out for 40 cycles after an initial denaturing at 96°C for 5 min. Each cycle consisted of denaturation at 96°C for 1 min, annealing at 58°C for 1 min and extension at 72°C for 1 min. After the final cycle of amplification, the extension was continued for an additional 7 min at 72°C. SSCP was performed using a DNA fragment analyser (GenePhor; Amersham Pharmacia Biotech, Uppsala, Sweden) at 600 V, 25 mA, 15 W and 5°C for 120 min, and the results were visualized by a DNA Silver Staining Kit (GenePhor; Amersham Pharmacia Biotech). To increase the quantity of mutant DNA before sequencing, extra bands that seemed to be migrating aberrantly from the SSCP gel were excised and reamplified for 25 cycles under the same conditions. The samples of aberrantly migrated bands in the SSCP gel were analysed for sequencing after the subsequent reaction. The sequence data were collected by ABI Prism 310 Collection Software and Sequence Navigator Software (Perkin Elmer, Norwalk, CT, USA).

mRNA QUANTIFICATION *VEGF*

Total RNA from 33 samples and three normal skeletal muscle samples was extracted using Trizol Reagent (Invitrogen Corporation, Carlsbad, CA, USA), according to the manufacturer's protocol. Five microgram of RNA from each sample were used for the subsequent reverse transcription. After the reaction, RNase treatment was performed to eliminate RNA.

Quantitative RT–PCR was performed using predeveloped *Taq*Man assay reagents (*VEGF*; Hs00173626_m1 glyceraldehyde-3-phosphate dehydrogenase (*GAPDH*): human GAPDH; Hs99999905_m1; Applied Biosystems, Foster City, CA, USA) and an ABI Prism 7700 Sequence Detection system (Applied Biosystems). The PCR reaction was carried out according to the manufacturer's protocol. The standard curve was constructed with serial dilutions of one of the cDNA samples of human normal skeletal muscle, and the data obtained were standardized using data of the international housekeeping gene, *GAPDH*. The final numerical value (V) in each sample was calculated as follows: V = *VEGF* mRNA/*GAPDH* mRNA value.

STATISTICAL ANALYSIS

A possible correlation between immunohistochemical expression of widespread β-catenin nuclear expression and VEGF was estimated by two-sided Fisher's exact test. *VEGF* mRNA expression levels according to the status of β-*catenin* mutation were compared by

Mann–Whitney *U*-test. Probability values <0.05 were considered significant.

Results

IMMUNOHISTOCHEMISTRY

Immunoreactivity of β-catenin was observed in the nuclei and cytoplasm of fibroblastic tumour cells (Figure 1). We defined more than 50% positive cells with nuclear imunoreactivity as widespread β-catenin nuclear staining (aberrant staining). The correlation of β-catenin and VEGF expression is summarized in Table 4. Thirty-five cases (56%) were judged as showing widespread β-catenin nuclear staining. There was no statistically significant correlation between the widespread nuclear staining of β-catenin and desmoid tumour location (abdominal, intra-abdominal or extra-abdominal). VEGF-positive cells also appeared to be scattered evenly throughout the section (Figure 2), and 47 cases (73%) showed overexpression of VEGF. For each location analysed individually (abdominal, intra-abdominal or extra-abdominal), there was no significant correlation between widespread β-catenin nuclear imunoreactivity and VEGF overexpression (Table 5). However, among all desmoid tumours, there was a statistically significant correlation between widespread β-catenin nuclear staining and VEGF overexpression ($P = 0.04$, Table 5).

Concerning recurrent tumours, all 11 samples from five cases showed widespread β-catenin nuclear imunoreactivity and VEGF overexpression. Four of five samples of primary tumours that went on to recur were positive for β-catenin, and all five primary samples were positive for VEGF. There was no statistically significant correlation between primary and recurrent tumours in widespread β-catenin nuclear staining, and there was no statistically significant difference between primary and recurrent tumours in VEGF overexpression.

Table 4. Immunohistochemistry in primary tumours

	β-catenin widespread nuclear staining	VEGF overexpression
Abdominal ($n = 12$)	7	8
Intra-abdominal ($n = 9$)	8	8
Extra-abdominal ($n = 42$)	20	31
Total ($n = 63$)	35 (56%)	47 (73%)

VEGF, vascular endothelial growth factor.

MICROVESSEL DENSITY

Microvessel density assessed by immunohistochemical staining of CD31 immunohistochemistryranged from 1.5 to 19.25/0.26 mm^2 [mean ± standard deviation (SD): 9.68 ± 4.26/0.26 mm^2]. MVD in recurrent tumours was significantly higher than that in primary tumours (mean ± SD: recurrent tumours, 13.97 ± 5.32; primary tumours, 9.56 ± 3.72; $P = 0.02$; Figure 3A) (recurrent case; Figure 4A, primary case; Figure 4B). MVD in VEGF-positive samples tended to be higher than that in VEGF-negative samples (mean ± SD VEGF expression (+), 10.62 ± 4.41; VEGF expression (−), 9.55 ± 3.96; Figure 3B); however, this difference was not statistically significant.

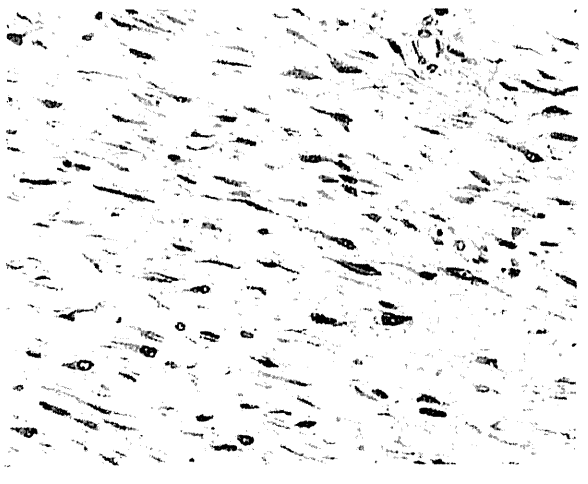

Figure 1. Immunohistochemistry of β-catenin.

Figure 2. Immunohistochemistry of vascular endothelial growth factor.

Table 5. Correlation between β-catenin widespread nuclear staining and vascular endothelial growth factor (VEGF) overexpression

	Abdominal		Intra-abdominal		Extra-abdominal		Total	
	VEGF (+)	VEGF (−)	VEGF (+)	VEGF (−)	VEGF (+)	VEGF (−)	VEGF (+)	VEGF (−)
β-catenin widespread nuclear staining								
(+)	6	1	7	1	17	3	30	5
(−)	2	3	1	0	14	8	17	11
	$P = 0.28$		$P = 1.0$		$P = 0.16$		$P = 0.04$	

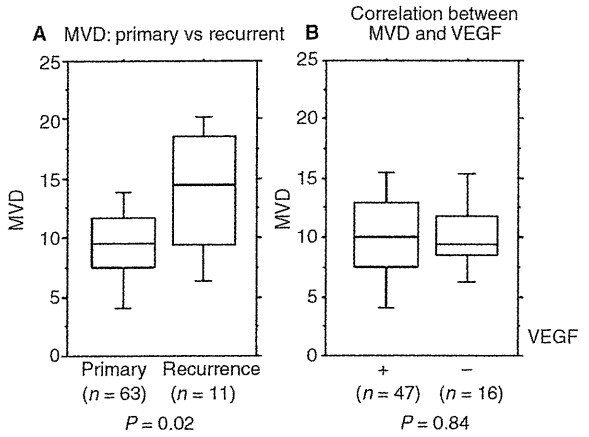

Figure 3. A, Microvessel density (MVD). MVD in recurrent tumours was higher than that in primary tumours ($P = 0.02$). B, There was no statistically significant difference between MVD in vascular endothelial growth factor (VEGF) overexpression samples and that in VEGF-negative samples ($P = 0.84$).

β-*CATENIN* GENE MUTATION

Single-strand conformation polymorphism analysis followed by DNA direct sequencing revealed β-*catenin* mutation in seven cases in frozen materials (12 of 33 samples). There were seven point mutations of 22 primary cases (32%), all of which were missense mutations. There was no statistically significant difference between tumour location and incidence of β-*catenin* mutation. All cases with β-*catenin* mutation showed immunohistochemical widespread β-catenin nuclear expression and VEGF overexpression. There was no statistically significant correlation between β-*catenin* mutation and VEGF overexpression ($P = 0.14$, Table 6).

QUANTITATIVE ASSAY FOR *VEGF* MRNA

The analysed primary tumours were divided into two groups according to the results of mutational analysis: a β-*catenin* mutated group and a β-*catenin* wild-type group. Figure 5 shows the boxplot of *VEGF* mRNA expression in the β-*catenin* mutated group and the β-*catenin* wild-type group (mutated group, 1.91 ± 0.85;

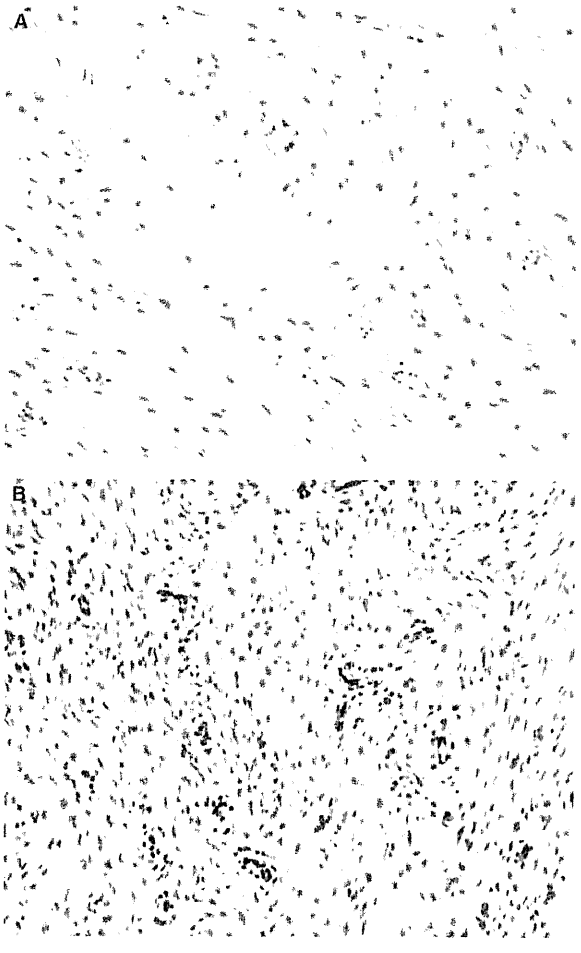

Figure 4. A, Extra-abdominal desmoid arising in the right shoulder of a 25-year-old female. Microvessel density (MVD) in primary lesion. B, Extra-abdominal desmoid arising in the right shoulder of a 25-year-old female. MVD in recurrent lesion.

Table 6. Immunohistochemistry in primary tumours

	VEGF overexpression (+)	VEGF overexpression (−)
β-catenin mutation (+)	7	0
β-catenin mutation (−)	10	5
Total	17	5

$P = 0.14$.

wild-type group 2.05 ± 1.04). According to the β-*catenin* mutation status, the *VEGF* mRNA expression level demonstrated no significant difference ($P = 0.96$, Figure 5).

Secondly, the analysed primary cases were divided into two groups according to the state of recurrence: a recurrent group and a non-recurrent group. Figure 6 shows the boxplot of *VEGF* mRNA expression in the recurrent group and the non-recurrent group (recurrent group, 1.90 ± 0.89; non-recurrent group 2.02 ± 1.07). There was no statistically significant difference between recurrent and non-recurrent groups ($P = 0.89$, Figure 6).

Discussion

We have investigated previously whether aberrant β-catenin expression correlates with cyclin D1 overexpression in desmoid tumours.[13] In the β-*catenin* mutated group, *cyclin* D1 mRNA expression was significantly higher than that in the β-*catenin* wild-type group.[14] We have reported recently that *MMP-7* is a target gene of the Wnt/β-catenin signalling pathway in desmoid tumours, which is one of the factors in recurrence.[3] However, angiogenesis also plays an essential role in tumour progression, and is regulated by VEGF.[5] In this study, we have demonstrated that widespread β-catenin nuclear expression correlates with VEGF overexpression in desmoid tumours, which suggests that VEGF is one of the candidates for the target genes of the Wnt/β-catenin signalling pathway in desmoid tumours.

We have compared MVD between primary and recurrent tumours and found that MVD in recurrent tumours is significantly higher than that in primary tumours. Yokoyama *et al.*[6] reported that high vascularity gives the tumour active growth potential. Choi *et al.*[15] reported that angiogenesis is essential for breast cancer progression and is regulated by VEGF, a target gene of the Wnt/β-catenin signalling pathway. The difference between MVD in VEGF overexpression samples and that in VEGF-negative samples was not significant. However, MVD in samples with VEGF-overexpression tended to be higher than that in VEGF-negative samples in the present study.

In the present study, β-*catenin* mutation was identified in seven of 22 samples (31%), while Amary *et al.* reported β-*catenin* mutation in 66 of 76 samples (87%) and Lazar *et al.* reported β-*catenin* mutation in 117 of 138 samples (85%).[4,16] We found a low ratio of

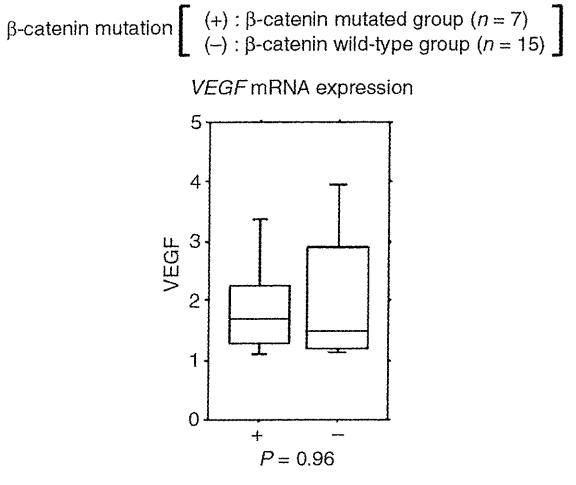

Figure 5. β-*catenin* mutation. There was no statistically significant difference between *VEGF* mRNA expression of the β-catenin mutated group and that of the wild-type group ($P = 0.96$).

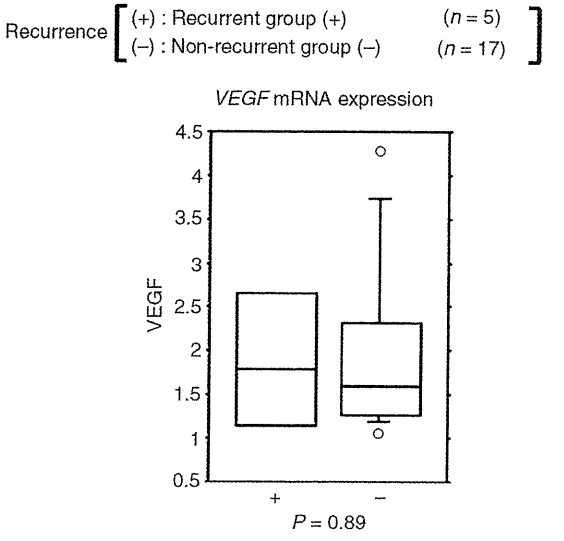

Figure 6. Recurrence. In the recurrent group, the *VEGF* mRNA expression levels demonstrated no significant difference ($P = 0.89$).

β-*catenin* mutation when we compared it with the mutational analysis of Amary and Lazar. One of the reasons for this may be that the methods of mutational analysis vary. Saito *et al.*,[13,14] using methods that are similar to ours, reported β-*catenin* mutation in seven of 18 samples (39%) and in three of 12 samples (25%). In another paper, β-catenin mutation was detected in seven of 19 samples (38%, Heinrich).[17] We may also need to consider differences between patient ethnicities. These show the data for oriental people as follows: Miyoshi (54%, 22 of 42), Saito (39%, seven of 18; 25%, three of 12) and Jilong (19%, 13 of 69).[13,14,18,19] Others show the data for westerners as follows: Amary (87%, 66 of 76), Lazar (85%, 117 of 138), Tejpar (52%, 22 of 42), Abraham (45%, 15 of 33) and Heinrich (38%, seven of 19).[4,16,17,20,21] Therefore, there may be differences between patient ethnicities.

We divided samples into two groups based on β-*catenin* mutational analysis: the β-*catenin* mutated group and the β-*catenin* wild-type group. Unfortunately, we could not find a correlation between β-*catenin* mutation and *VEGF* mRNA expression. However, all cases with β-*catenin* mutation showed widespread immunohistochemical β-catenin nuclear expression and VEGF overexpression. In fact, the results suggested that VEGF plays an important role in infiltrative growth.

We found no significant difference between the recurrent and the non-recurrent groups with respect to the *VEGF* mRNA level. However, in recurrent desmoid tumours there was high MVD and high vascularity, suggesting that angiogenesis is an important factor in tumour recurrence.

In conclusion, in desmoid tumours, widespread β-catenin nuclear expression correlated with VEGF overexpression, and MVD in recurrent tumours was significantly higher than that in primary tumours.

Acknowledgements

This work was supported by a Grant-in-Aid for Scientific Research (B) from the Japan Society for the Promotion of Science, Tokyo, Japan (no. 21390107). The English used in this manuscript was revised by KN International.

References

1. Lewis JJ, Boland PJ, Leung DH, Woodruff JM, Brennan MF. The enigma of desmoid tumors. *Ann. Surg.* 1999; **229**; 866–872.
2. Tejpar S, Michils G, Denys H *et al.* Analysis of Wnt/Beta catenin signalling in desmoid tumors. *Acta Gastroenterol. Belg.* 2005; **68**; 5–9.
3. Matono H, Oda Y, Nakamori M *et al.* Correlation between beta-catenin widespread nuclear expression and matrix metalloproteinase-7 overexpression in sporadic desmoid tumors. *Hum. Pathol.* 2008; **39**; 1802–1808.
4. Lazar AJ, Tuvin D, Hajibashi S *et al.* Specific mutations in the beta-catenin gene (CTNNB1) correlate with local recurrence in sporadic desmoid tumors. *Am. J. Pathol.* 2008; **173**; 1518–1527.
5. Khosravi SP, Fernandez PI. Tumoral angiogenesis: review of the literature. *Cancer Invest.* 2008; **26**; 104–108.
6. Yokoyama R, Shinohara N, Tsuneyoshi M, Masuda S, Enjoji M. Extra-abdominal desmoid tumors: correlations between histologic features and biologic behavior. *Surg. Pathol.* 1989; **1**; 29–42.
7. Ilysa M. Wnt signalling and the mechanistic basis of tumour development. *J. Pathol.* 2005; **205**; 130–144.
8. Goldblum J, Fletcher JA. Desmoid-type fibromatoses. In Fletcher CDM, Unni KK, Mertens F eds. *World Health Organization classification of tumour. Pathology and genetics: tumours of soft tissue and bone.* Lyon, France: International Agency for Research on Cancer (IARC), 2002; 83–84.
9. Machin P, Catasus L, Pons C, Munoz J, Matias GX, Prat J. CTNNB1 mutations and beta-catenin expression in endometrial carcinomas. *Hum. Pathol.* 2002; **33**; 206–212.
10. Oda Y, Yamamoto H, Tamiya S *et al.* CXCR4 and VEGF expression in the primary site and the metastatic site of human osteosarcoma: analysis within a group of patients, all of whom developed lung metastasis. *Mod. Pathol.* 2006; **19**; 738–745.
11. Kaya M, Wada T, Akatsuka T *et al.* Vascular endothelial growth factor expression in untreated osteosarcoma is predictive of pulmonary metastasis and poor prognosis. *Clin. Cancer Res.* 2000; **6**; 572–577.
12. Iwao K, Nakamori S, Kameyama M *et al.* Activation of the beta-catenin gene by interstitial deletions involving exon 3 in primary colorectal carcinomas without adenomatous polyposis coli mutations. *Cancer Res.* 1998; **58**; 1021–1026.
13. Saito T, Oda Y, Tanaka K *et al.* Beta-catenin nuclear expression correlates with cyclin D1 overexression in sporadic desmoid tumours. *J. Pathol.* 2001; **195**; 222–228.
14. Saito T, Oda Y, Kawaguchi K *et al.* Possible association between higher beta-catenin mRNA expression and mutated β-catenin in sporadic desmoid tumors: real-time semiquantitative assay by TaqMan polymerase chain reaction. *Lab. Invest.* 2002; **82**; 97–103.
15. Choi WW, Lewis MM, Lawson D *et al.* Angiogenic and lymphangiogenic microvessel density in breast carcinoma: correlation with clinicopathologic parameters and VEGF-family gene expression. *Mod. Pathol.* 2005; **18**; 143–152.
16. Amary MF, Pauwels P, Meulemans E *et al.* Detection of beta-catenin mutations in paraffin-embedded sporadic desmoid-type fibromatosis by mutation-specific restriction enzyme digestion (MSRED): an ancillary diagnostic tool. *Am. J. Surg. Pathol.* 2007; **31**; 1299–1309.
17. Heinrich MC, McArthur GA, Demetri GD *et al.* Clinical and molecular studies of the effect of imatinib on advanced aggressive fibromatosis (desmoid tumor). *J. Clin. Oncol.* 2006; **24**; 1195–1203.
18. Miyoshi Y, Iwao K, Nawa G, Yoshikawa H, Ochi T, Nakamura Y. Frequent mutations in the beta-catenin in desmoid tumors from patients without familial adenomatous polyposis. *Oncol. Res.* 1998; **10**; 591–594.

19. Jilong Y, Jian W, Xiaoyan Z, Xiaoqiu L, Xiongzeng Z. Analysis of APC/beta-catenin genes mutations and Wnt signalling pathway in desmoid-type fibromatosis. *Pathology* 2007; **39**; 319–325.
20. Tejpar S, Nollet F, Li C *et al.* Predominance of beta-catenin mutations and beta-catenin dysregulation in sporadic aggressive fibromatosis (desmoid tumor). *Oncogene* 1999; **18**; 6615–6620.
21. Abraham SC, Reynolds C, Lee JH *et al.* Fibromatosis of the breast and mutations involving the APC/beta-catenin pathway. *Hum. Pathol.* 2002; **33**; 39–46.

Skeletal Radiol (2011) 40:1487–1490
DOI 10.1007/s00256-011-1173-8

CASE REPORT

Bizarre parosteal osteochondromatous proliferation with an inversion of chromosome 7

Akio Sakamoto · Sumitada Imamura · Yoshihiro Matsumoto · Katsumi Harimaya · Shuichi Matsuda · Yusuke Takahashi · Yoshinao Oda · Yukihide Iwamoto

Received: 30 November 2010 / Revised: 5 April 2011 / Accepted: 6 April 2011 / Published online: 21 April 2011

Abstract Bizarre parosteal osteochondromatous proliferation (BPOP) is a benign exophytic proliferative lesion that predominantly involves the small tubular bones of the hands and feet. Histologically BPOP is characterized by a heterogeneous mixture of cartilage, bone and fibrous tissue. Recently, a translocation between chromosomes 1 and 17, or its variant translocations, has been reported to be unique in BPOP. The case of a 59-year-old woman with BPOP in the middle phalanx of the ring finger with increasing mass is reported herein. Computed tomography and magnetic resonance imaging depicted the central part of the exophytic bone lesion as having continuity to the underlying bone marrow, which is considered to be the typical finding of osteochondroma, but not a common finding in BPOP. In addition, an inversion of chromosome 7 [inv (7)(q22q32)] was observed. Therefore, this case suggests that the translocation between chromosomes 1 and 17 reported in other cases may not be the only cause of BPOP.

Keywords Bizarre parosteal osteochondromatous proliferation (BPOP) · Ring finger · Chromosomal abnormality · Computed tomography · Magnetic resonance imaging

A. Sakamoto (✉) · S. Imamura · Y. Matsumoto · K. Harimaya · S. Matsuda · Y. Iwamoto
Department of Orthopaedic Surgery,
Graduate School of Medical Sciences, Kyushu University,
Fukuoka 812–8582, Japan
e-mail: akio@med.kyushu-u.ac.jp

Y. Takahashi · Y. Oda
Department of Anatomic Pathology,
Graduate School of Medical Sciences, Kyushu University,
Fukuoka 812–8582, Japan

Introduction

Bizarre parosteal osteochondromatous proliferation (BPOP) is also known as Nora's lesion and was first described in 1983 [1]. BPOP is an exophytic bone lesion originating from the cortical surface and is characterized by a heterogeneous mixture of cartilage plus bone and fibrous tissue. The lesion predominantly involves the small tubular bones of the hands and feet [2]. BPOP is reported to have a tendency to recur. Radiologically, BPOP has a distinct margin from the cortical surface of the affected bone. Continuity of the central part of the lesion to the bone marrow of the host bone as seen in typical osteochondroma is not usually observed in BPOP [3, 4], although a corticomedullary continuity has been reported in several prior cases [5–8].

Whether BPOP is a reactive proliferative lesion or a neoplastic lesion remains controversial. BPOP may be related to trauma based upon a report showing that there was a history of trauma in 30% of cases that ranged from 2 months to 3 years before presentation of the lesion [2]. In addition, the histological features of BPOP are those of a reactive lesion. However, its aggressive growth clinically suggests a neoplasm. Moreover, the reported chromosomal abnormalities support the neoplastic nature of BPOP [9–11].

In the current report, we present an interesting case of BPOP with corticomedullary continuity to the host bone depicted by computed tomography (CT) and magnetic resonance imaging (MRI) as well as chromosomal analysis showing an inversion of chromosome 7.

Case report

Two months prior to her first visit to our institute, a 59-year-old woman noticed swelling of the distal ring finger. She was

Fig. 1 Plain radiograph showing an oval shaped exophytic bone lesion arising from the distal part of the middle phalanx (*left*). During the course of 4 months, the size of the tumor increased (*right*)

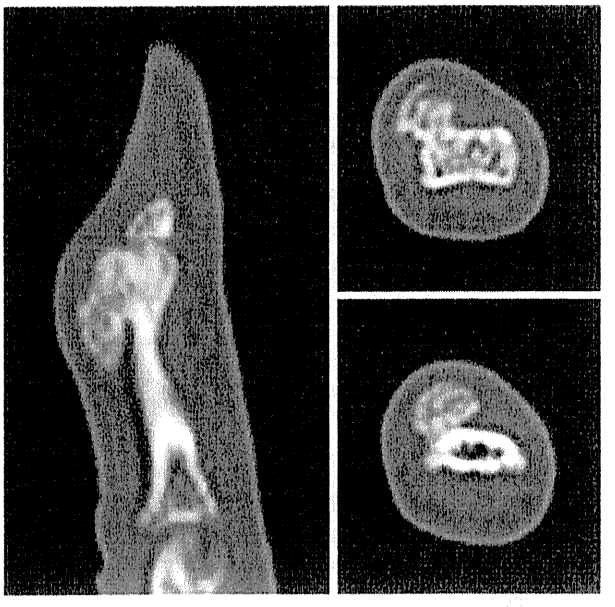

Fig. 3 CT depicts an exophytic bone lesion with continuity to the bone marrow of the host bone as well as cortical continuity

referred to our institute upon diagnosis of a bone tumor by her local hospital. She stated that she had experienced no episode of trauma. Clinical examination revealed a hard mass on the ulnar side at the level of the distal phalangeal joint of the left ring finger. Mobility of the lesion to the middle phalanx was not observed. Radiographs showed an exophytic lesion with a clear margin originating from the surface of the distal middle phalanx (Fig. 1). Periosteal bone formation was not observed. The size of the mass on the radiograph was 7.5 × 4.4 mm. MRI showed a lesion with low intensity on T1-weighted imaging, which was adjacent to the proximal phalanx. The lesion had heterogeneous signal intensity covered by a high-signal intensity area on T2-weighted imaging (Fig. 2). During the course of 4 months—6 months after the lesion was initially noticed——the size of the tumor had enlarged to 10.0 × 5.0 mm (Fig. 1). CT showed an exophytic bone lesion arising from the phalanx. The cortex of the host bone continued to the lesion without a border at the base. The central part of the lesion had continuity with the underlying bone marrow of the host bone (Fig. 3). Adjacent to the base, a clear zone between the lesion and the host bone was observed.

Based upon a clinical diagnosis of BPOP, resection of the tumor was performed. The surface of the lesion was covered by fibrous tissue. The resection included the surrounding fibrous tissue and the adjacent host bone. Histopathology of the lesion showed three components: cartilage, bone, and spindle cells (Fig. 4a). Irregular ossification was seen in the cartilage and bone tissue, which formed bone trabeculae (Fig. 4b). The bone

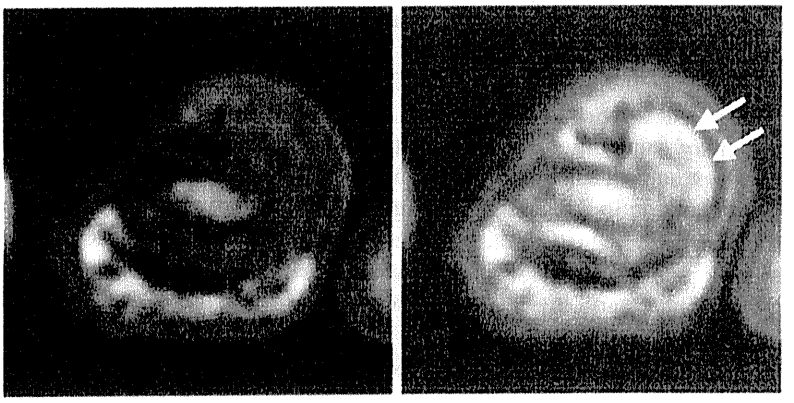

Fig. 2 A T1-weighted MRI image shows a low intensity mass adjacent to the proximal phalanx (*left*). A T2-weighted image shows the lesion has heterogeneous signal intensity with coverage of a high intensity area (*arrows*) (*right*)